IEEE Access
Multidisciplinary | Rapid Review | Open Access Journal

Received October 1, 2020, accepted October 21, 2020, date of publication October 26, 2020, date of current version November 10, 2020.

Digital Object Identifier 10.1109/ACCESS.2020.3033622

Numerical Analysis of Tube Expansion by Electromagnetic Forming Using Magnetic Field Shaper

LI QIU[1,2], (Member, IEEE), CHENGLIN WANG[1], AHMED ABU-SIADA[3], (Senior Member, IEEE), WANG BIN[1], ZHANG WANG[1], WEIKANG GE[1], CHANG LIU[1], AND YUWEI FAN[1]

[1]College of Electrical Engineering and New Energy, China Three Gorges University, Yichang 443002, China
[2]Hubei Provincial Key Laboratory of Operation and Control of Cascade Hydropower Stations, Yichang 443002, China
[3]Department of Electrical and Computer Engineering, Curtin University, Perth, WA 6102, Australia

Corresponding authors: Chenglin Wang (1361145341@qq.com) and Yuwei Fan (522178398@qq.com)

This work was supported in part by the National Natural Science Foundation of China under Grant 51877122 and Grant 51707104, and in part by the Research Fund for Excellent Dissertation of China Three Gorges University under Grant 2019SSPY065.

ABSTRACT Uneven axial deformation is the current main issue of the tubes electromagnetic bulging technology which calls for innovative and cost-effective solutions. This paper presents a new method to overcome the above-mentioned issue based on employing a magnetic field shaper. The proposed magnetic field shaper is employed in the middle of the pipe and the driving coil. Induced eddy current control is realized by changing the structural parameters of the magnetic field shaper; thereby regulating the electromagnetic force distribution. The effectiveness of the proposed method is investigated through numerically comparing the electromagnetic performance of two EMF setups; traditional coil-based loading model and magnetic field shaper driving coil-based loading model proposed in this paper. The influence of the magnetic field shaper structural parameters on the tube electromagnetic forming performance is examined for optimum structure design. Results reveal that the concave profile of the radial electromagnetic force in the traditional loading method can be effectively improved using the proposed loading in this paper. The introduction of a magnetic field shaper not only changes the induced eddy current distribution, but also regulates the electromagnetic force profile in the axial-direction of the pipe which effectively enhances the uniform range of the pipe electromagnetic bulging, the maximum uniform deformation area is increased from 9mm to 35mm.

INDEX TERMS Electromagnetic forming, Lorentz force distribution, magnetic field shaper, numerical simulation, uniformity.

I. INTRODUCTION

Electromagnetic forming (EMF) is a technology that employs electromagnetic-force pulsation to realize metallic workpiece processing [1]–[3]. Compared with conventional mechanical-based processing, EMF can improve plastic deformation ability of materials and enhance their forming limit about 5 to 10 times due to its high strain rate (10^3-$10^5 s^{-1}$) [4]–[6]. Because the electromagnetic force is of a non-contact nature [7], [8], EMF is able to improve the surface quality of the formed workpiece [9]–[11].

Based on the processing object [12], [13], EMF is divided into tube or plate type process [14]–[16]. In both types, uniformity of workpiece deformation has been a sustained issue that has not been fully resolved yet regardless the several attempts presented in the literature [17], [18]. For example, a concave driving coil is proposed in [19]. While this type of coil could improve the uniformity of tube axial forming, its complex structure may make it infeasible for practical implementation. A uniform pressure coil is proposed in [20] to generate uniform electromagnetic force at the center of the sheet workpiece. This technique could rectify the uneven electromagnetic force of traditional sheet EMF and has been successfully used for mobile phone sheet processing. An electromagnetic gradual bulging process of tube is presented in [21] in which driving coils are located at the two ends along with the middle of the pipe. Investigating the influence of various overlap ratios on the forming uniformity shows that there is an optimum overlap ratio of the coils at which the electromagnetic gradual bulging of the pipe achieves the

The associate editor coordinating the review of this manuscript and approving it for publication was Mehmet Alper Uslu.

best uniformity. In [22], the influence of a stepped magnetic collector on the axial deformation of a workpiece is analyzed. Simulation and experimental analyses revealed that the radial electromagnetic force of the stepped magnetic collector is approximately 23 to 85% more than that when a conventional driving coil is directly used. A 3D model was developed in [23] to analyze the electromagnetic field profile in an EMF system with a magnetic concentrator. Reported results showed that the magnetic concentrator can improve the magnetic field profile and its uniformity in a specific area. Reference [24] introduced a magnetic concentrator into an electromagnetic welding system to increase the magnetic field strength and achieve a relatively uniform electromagnetic force distribution. In [25], it was found that the distance between the coil and the plate side wall during molding process is too far which resulted in inadequate electromagnetic force on the side wall. As such, a cylindrical tube magnetizer is proposed in [25] to enhance the electromagnetic force exerted on the side wall has been increased by about 10 times; achieving a maximum deformation of 1.18 mm as per the reported results. A new separable field forming machine design is proposed in [26] for electromagnetic sheet metal impact forming. Results showed that the Lorentz force can be concentrated on a local area of the workpiece which makes it possible to control the magnetic field pressure distribution through a proper design of the magnetic concentrator.

In general, the issue of the workpiece uneven axial deformation can be solved through the selection of proper structure design and placement of the driving-coil [20]–[25]. However, winding up particular driving coil structures is difficult and may involve high cost as well. The introduction of a magnetic concentrator in the literature was mainly to strengthen the magnetic field and electromagnetic-force on a specific area with no evidence so far for improving the entire deformation uniformity of the workpiece.

Based on the above discussion, the key contribution of this article is to:

- suggest a tube electromagnetic bulging process based on magnetic field shapers to improve the pipe deformation in the axial direction.
- present a precise model for the proposed EMF topology.
-investigate the effect of the inner and outer wall heights of the magnetic field shaper on the pipe EMF performance.
- numerically compare the performance of the proposed EMF topology with the traditional method.

II. BASIC PRINCIPLES AND MAGNETIC FIELD SHAPER COIL

A. BASIC PRINCIPLES

The traditional tube EMF system consists of a capacitor that acts as a pulsation power supply through a discharging switch to the main driving coil and the formed tube as shown in Fig. 1 [27]–[29]. The generated pulse current within the coil results in an induced eddy current in the tube. As a result, a huge electromagnetic force is produced that drive the tube at high speed to perform the required bulging [29]. Magnetic field shaper is an important auxiliary tool in the electromagnetic forming process, as it can adjust the electromagnetic field distribution profile. However, the conventional magnetic field shaper concentrates the electromagnetic energy on a specific area to increase the electromagnetic force on this particular area.

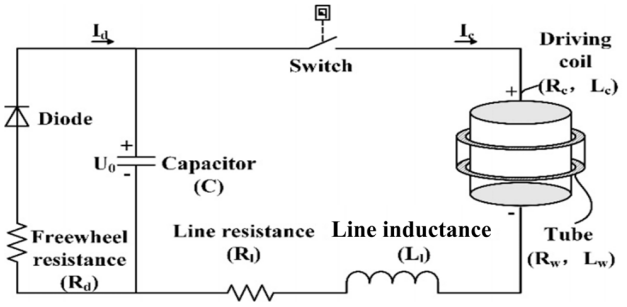

FIGURE 1. Traditional electromagnetic forming system [29].

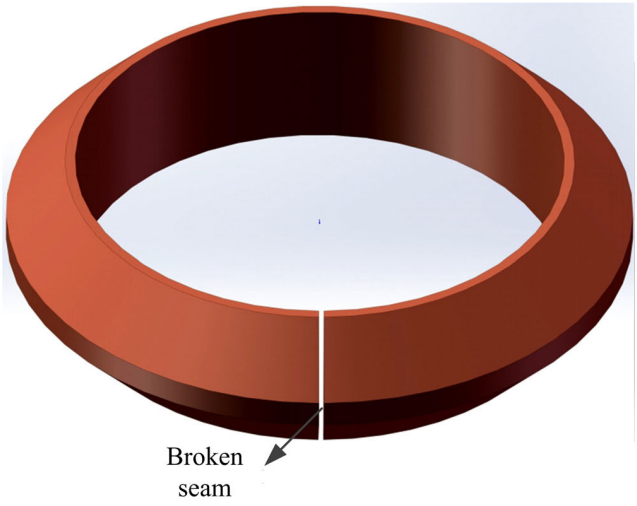

FIGURE 2. Structure diagram of traditional magnetic field shaper.

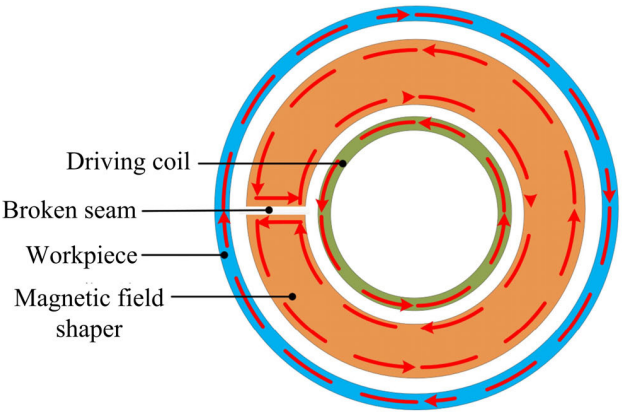

FIGURE 3. Top view of electromagnetic bulging of traditional magnetic field shaper tube.

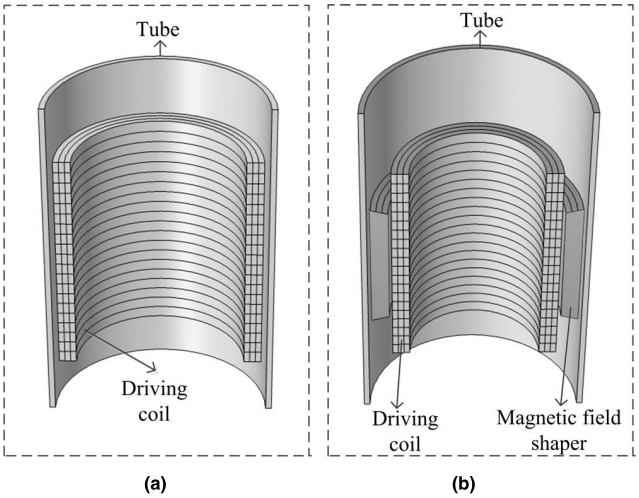

FIGURE 4. Geometrical model of electromagnetic bulging of tube: (a) traditional coil; (b) magnetic field shaper coil.

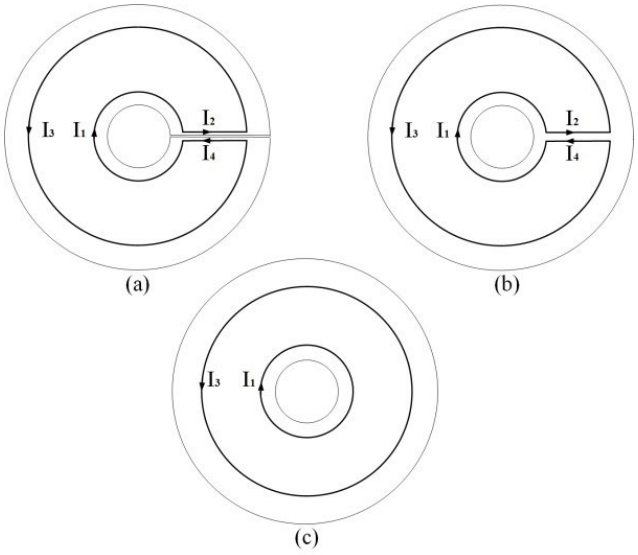

FIGURE 5. Simplification process of the magnetic field shaper model: (a) Initial 3Dmodel; (b) Filled model; (c) Simplified 2D model.

Fig. 2 shows the structural diagram of a traditional magnetic field shaper currently used for tubes electromagnetic bulging. As can be see, the magnetic field shaper is structured on the form of a circular ring with a trapezoidal cross section with a very small gap. The height of the inner wall of the ring is much greater than the height of the outer wall. Fig. 3 shows a top-side view of the pipe EMF with the traditional magnetic field shaper.

In this method, the capacitor discharges stored energy into the driving coil to generate a counterclockwise pulsing current. According to the law of electromagnetic induction, a clockwise induced current passe through the inner wall of the magnetic field shaper which encounters a gap as shown in Fig. 3. Therefore, the induced current flows along the broken seam to the outer wall of the magnetic converter. Hence, a counterclockwise induced current is formed on the outer wall which acts as an excitation source and induces current inside the workpiece. Thereby generating pulse electromagnetic force to drive the workpiece to deform. Since the height of the outside-wall of the magnetic field shaper is much smaller than the inside-wall and the current flowing through both walls are equal, then the current density on the outside-wall of the magnetic field shaper is much greater than that of the inside-wall. The field shaper works like a magnifying glass: directing, intensifying, and shaping the magnetic field into a homogeneous distribution.

B. PROPOSED MAGNETIC FIELD SHAPER DESIGN

The traditional magnetic field shaper is mainly used to increase the electromagnetic force at particular area of the workpiece. This paper extends the functionality of the magnetic field shaper to achieve deformation uniformity of the entire workpiece. The conventional electromagnetic bulging model is as shown in Fig. 4(a) in which the driving coil is located within the pipe that has more height than the driving coil [3]. In the traditional method, the uneven axial distribution of the radial electromagnetic force results in a convex tube profile which is referred as end effect. At the same time, the end material is constrained by the static part during the deformation process, and the deformation becomes more difficult, which eventually leads to uneven deformation of the pipe in the axial direction.

In order to solve poor quality issue of the tube expansion caused by the axial non-uniformity of the radial electromagnetic force, this paper proposes a magnetic field shaper-based structure as shown in Fig. 4(b). In this model, the magnetic field shaper is located among the driving coil and the tube. Due to the difference of the current densities on the outside and inside walls of the magnetic field shaper, the magnetic field strength at the middle of the tube is getting weaker. By changing the structural parameters of the magnetic-field converter, the tube induced eddy current can be adjusted to a certain extent, so as to realize the loading of different electromagnetic force distributions, increase the radial forming amount of the end of the pipe, and improve the pipe's uniformity.

III. ELECTROMAGNETIC-STRUCTURE COUPLING MODEL

EMF is a complex dynamic deformation process, which involves strong coupling between different fields including electromagnetic, mechanical and thermal. In order to better understand the effect of each physical field on the EMF process, finite element analysis is utilized. In order to simplify the simulation model without compromising the model's accuracy, this paper proposes a two-dimensional simulation model to replace the complex traditional three-dimensional simulation model. This simplification is explained below.

The induced eddy current in the magnetic field shaper can be divided into four equal current components: inner wall current I_1, I_2 on one side of the air gap, outer wall

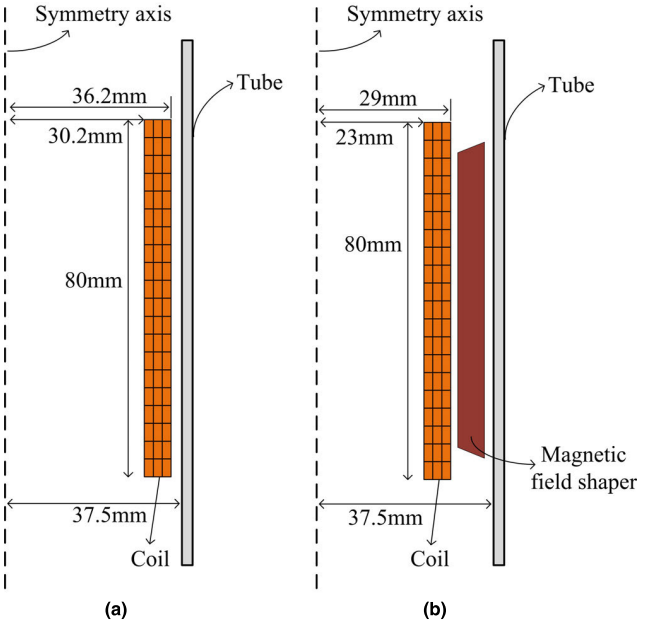

FIGURE 6. Physical structure of the EMF using (a) conventional cylindrical coil, (b) the proposed magnetic field shaper.

current I_3 and I_4 on the other side of the air gap, as shown in Figure 5(a). In order to simplify the model, the air gap of the magnetic field shaper is firstly assumed to be filled with the same material, as shown in Figure 5(b). Because the distance between the two equal currents I_2 and I_4 that flow in opposite direction is small [30], the magnetic field generated is only confined near the gap, and will have little impact on the electromagnetic bulging of the entire pipe. Therefore, the model can be simplified further as shown in Figure 5(c) of which all parameters including the magnetic field and induced currents will have axial symmetry. This, the three-dimensional model can be replaced by a simplified two-dimensional model. In [30], the equivalent process of the magnetic field shaper is presented in details.

COMSOL software is employed to develop the electromagnetic-structure coupling 2D axisymmetric model of the pipe EMF process.

The detailed geometrical structure of the proposed model is shown in Figure 6 and is briefly elaborated below.

Figure 6(a) shows the electromagnetic pipe bulging of the traditional spiral coil. The coil has 3 layers, 20 turns each with inner radius of 30.2mm and outer radius of 36.2 mm. Figure 6(b) shows the electromagnetic bulging of tube based on a magnetic field shaper. The coil has also 3 layers of 20 turns each and inner radius of 23mm and outer radius of 29mm. All coils are made of copper wires with a cross-sectional area 2mm x 4mm and 80 mm height.

The height of the inner wall H_i and outer wall H_o of the magnetic field shaper are the geometric variables investigated in the below sections of this article. The magnetic field shaper is of 6mm thickness and it is placed coaxially between the pipe and the coil with side spacing of 1.25mm. The converter is made of high-conductivity bronze or copper material.

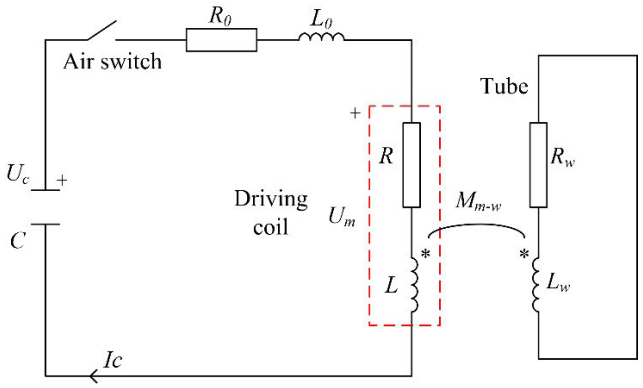

FIGURE 7. Equivalent discharge circuit of the tube electromagnetic forming without magnetic field shaper.

TABLE 1. Circuit parameters.

Symbol	Description	Value
Circuit		
C_0	Capacitance	320μF
U_0	Discharge voltage	6.4kV
R_0	Line resistance	35mΩ
L_0	Line inductance	12μH
R_d	Crowbar resistance	0. 2Ω
S	Cross sectional area of the wire	2mm×4mm

The workpiece considered in this paper is an AA5083-O round aluminum alloy pipe fitting with inner radius of 37.5mm, 39.5mm outer radius and a height of 130mm.

A. CIRCUIT ANALYSIS OF THE EMF SYSTEM

The electromagnetic analysis in the pipe bulging process is based on the equivalent circuit. Due to the generated high temperature during the EMF process, a discharge circuit with a crowbar resistor is usually used to dissipate the temperature rise of the coil through the crowbar resistor. The discharge circuit can be modeled as a second-order RLC zero input circuit. The circuit includes capacitor bank (C), line resistance (R_0), line inductance (L_0), driving coil equivalent parameters (R, L) and the workpiece equivalent parameters (R_w, L_w). These parameters are given in Table 1. When there is no magnetic field shaper, the equivalent discharge circuit of the traditional pipe electromagnetic bulging is as shown in Figure 7.

According to Kirchhoff's law:

$$\begin{cases} \boldsymbol{U_c} = \boldsymbol{U}_l + \boldsymbol{U}_{coil} \\ \boldsymbol{U}_l = R_0 \boldsymbol{I_c} + L_0 \dfrac{d\boldsymbol{I_c}}{dt} \\ \boldsymbol{U}_{coil} = R\boldsymbol{I_c} + L\dfrac{d\boldsymbol{I_c}}{dt} + M_{m-w}\dfrac{d\boldsymbol{I_w}}{dt} \\ \boldsymbol{U_c} = \boldsymbol{U_0} - \dfrac{1}{C}\displaystyle\int_0^t \boldsymbol{I_c} dt \end{cases} \tag{1}$$

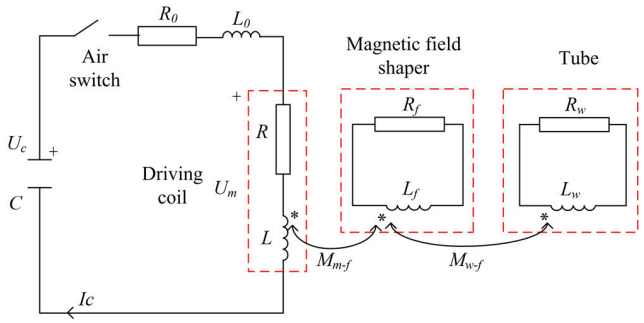

FIGURE 8. Equivalent discharge circuit of the tube electromagnetic forming with magnetic field shaper.

$$\begin{cases} \boldsymbol{I}_{\text{coil}} + \boldsymbol{I}_{\text{c}} - \boldsymbol{I_d} = 0 \\ R_{\text{w}}\boldsymbol{I_w} + L_w \dfrac{d\boldsymbol{I_w}}{dt} + M_{w-m}\dfrac{d\boldsymbol{I}_c}{dt} = 0 \end{cases} \tag{2}$$

$$\begin{cases} \boldsymbol{I_d} = 0 \; U_{\text{c}} \geq 0 \\ \boldsymbol{I_d} = \dfrac{\boldsymbol{U_c}}{R_d} U_{\text{c}} < 0 \end{cases} \tag{3}$$

When there is a magnetic field shaper in the discharge circuit, direct coupling between the driving coil and the tube is ignored and the equivalent circuit is as shown in Figure 8. For this circuit, (2) is modified to:

$$\begin{cases} \boldsymbol{I}_{\text{coil}} + \boldsymbol{I}_{\text{c}} - \boldsymbol{I_d} = 0 \\ R_f\boldsymbol{I}_f + L_f \dfrac{d\boldsymbol{I}_f}{dt} + M_{f-m}\dfrac{d\boldsymbol{I}_c}{dt} + M_{f-w}\dfrac{d\boldsymbol{I}_w}{dt} = 0 \\ R_{\text{w}}\boldsymbol{I_w} + L_w \dfrac{d\boldsymbol{I_w}}{dt} + M_{w-f}\dfrac{d\boldsymbol{I}_f}{dt} = 0 \end{cases} \tag{4}$$

In these equations, U_c is the capacitor voltage, U_o is the capacitor voltage at the initial state, U_1 is the line voltage of the discharge circuit, $\boldsymbol{I_d}$ is the current in the freewheeling circuit, $\boldsymbol{I_{coil}}$ is the driving coil current, $\boldsymbol{I_w}$ is the induced eddy current in the pipe.

B. MAGNETIC FIELD ANALYSIS

The pulse current of the driving coil is determined by equations 1 through 4. When a time-varying pulse current passes through the forming coil, a time-varying magnetic field is generated in the vicinity of the coil that can be expressed by the below equations.

$$\nabla \times \boldsymbol{H} = \boldsymbol{J} \tag{5}$$

$$\nabla \times \boldsymbol{E_\varphi} = -\frac{\partial \boldsymbol{B_z}}{\partial t} + \nabla \times (\boldsymbol{v_z} \times \boldsymbol{B_r}) \tag{6}$$

$$\nabla \cdot \boldsymbol{B} = 0 \tag{7}$$

$$\boldsymbol{J_\varphi} = \frac{\boldsymbol{I_{coil}}}{s} = \gamma \boldsymbol{E_\varphi} \tag{8}$$

where $\boldsymbol{B}$ is the magnetic flux density; $\boldsymbol{E}$ is the electric field intensity; $\boldsymbol{v}$ is the pipe fitting speed which is 0 at the initial state, $\boldsymbol{J}$ is the induced eddy current density; γ is the pipe conductivity. The subscripts r, φ, and z represent the radial, hoop and axial components of the vector; respectively. The electromagnetic force density $\boldsymbol{F}$ is calculated using (9).

$$\boldsymbol{F} = \boldsymbol{J} \times (\nabla \times \boldsymbol{A}) \tag{9}$$

TABLE 2. Material parameters of tube.

Symbol	Description	Value
Workpiece		
R_{in}	Inner-diameter	75 mm
R_{out}	Outer-diameter	79 mm
H_w	Height	130mm
μr	Relative permeability	1
ε	Relative permittivity	1
ρ	Mass density	2700 kg/m^3
σ	Conductivity	3.03e7 S/m
γ	Poisson ratio	0.33
E	Young modulus	70 GPa
σ_{ys0}	Initial-yield stress	32.6 MPa

The model established in this paper has axial symmetry. Therefore, the induced eddy current has only a circumferential direction, and the electromagnetic force density is calculated from:

$$\boldsymbol{F_z} = \boldsymbol{J_\varphi} \times \boldsymbol{B_r} \tag{10}$$

$$\boldsymbol{F_r} = \boldsymbol{J_\varphi} \times \boldsymbol{B_z} \tag{11}$$

where $\boldsymbol{F_z}$ and $\boldsymbol{F_r}$ are the axial and radial electromagnetic force densities of the pipe; respectively. $\boldsymbol{J_\varphi}$ is the induced eddy current in the circumferential direction of the pipe.

C. MECHANICAL FIELD ANALYSIS

When the pulsing current flows through the coil, the electromagnetic force generated under the combined action of the induced eddy current and the magnetic field strength drives the pipe to deform. Therefore, it is necessary to make a detailed analysis of the mechanical field of the tube. In the model developed in this paper, the pipe fitting is an annealed 5083 pure aluminum alloy with detailed parameters listed in Table 2.

The dynamic process of the pipe bulging can be expressed by the following equation:

$$\rho \frac{\partial^2 \boldsymbol{u}}{\partial t^2} - \nabla \bullet \boldsymbol{\sigma} = \boldsymbol{F} \tag{12}$$

where ρ is the tube density; u is the displacement vector which is 0 in the initial state, σ is the stress tensor and F is the electromagnetic force density.

It is worth noting that the material properties of aluminum alloy changes with the strain rate [27]. Usually, the forming speed reaches 180 to 300m/s [30]. Therefore, it is necessary to consider the effect of high speed and high strain rate on

the material properties of the tube. In this paper, Cowper-Symonds material constitutive model is used to simulate AA5083-O tube based on (13) [31].

$$\sigma = [1 + (\frac{\varepsilon_{pe}}{P})^m]\sigma_{ys} \tag{13}$$

where σ is the flow stress of the pipe material under high-speed deformation, P is the viscosity of the pipe material, m is the strain rate hardening of the material, and σ_{ys} is the flow stress under quasi-static conditions. Under normal circumstances, $P = 6500$ and $m = 0.25$ [31].

In [19], the authors have used this model to study the free electromagnetic bulging of tube with concave coils. Obtained simulation results were in good agreement with the experimental ones which attests the high accuracy of the simulation model.

IV. SIMULATION ANALYSIS

The induced eddy current and the strength of the magnetic field together determine the electromagnetic force experienced by the pipe. When the system parameters remain unchanged, the distribution of the radial electromagnetic force will be the main parameter affecting the uniformity of the axial deformation of the pipe. Therefore, this section investigates the electromagnetic bulging of the pipe from the following two aspects.

A. RADIAL-ELECTROMAGNETIC FORCE AND TUBE WALL DEFORMATION BEHAVIOR

In order to examine the radial electromagnetic-force acting in the axial direction of the pipe along with the deformation behavior of the pipe, two design parameters of the magnetic field shaper are varied; these are: the inner wall height H_i which is changed from 42mm to 49mm, with a step change of 1mm and the outer wall height H_o that is changed in the range 45mm-53mm in a 1mm step change. At the initial state, Hi is42mm, and Ho is 45 mm.

1) INFLUENCE OF H_i

Figure 9(a) shows the influence of the height of the inner wall of the magnetic field shaper on the radial-electromagnetic force. It can be seen that the radial electromagnetic force on the pipe at the area corresponding to the outer wall of the magnetic field shaper is uniformly distributed and has the same value regardless the value of H_i, and attenuation phenomenon occurs at the end of the magnetic field shaper. With the increase of H_i, the radial electromagnetic force on the middle section of the tube increases uniformly, while the electromagnetic force at the end of the magnetic field shaper is obviously weakened. Therefore, changing H_i can effectively regulate the radial electromagnetic force profile on the tube. Fig. 9(b) depicts the effect of H_i on the deformation behavior. It can be seen that with the increase of the height of the inner wall, the forming profile in the axial direction of the pipe changes from concave to convex. At the point of transition, corresponding to 46mm, the best uniform expansion of the pipe can be attained.

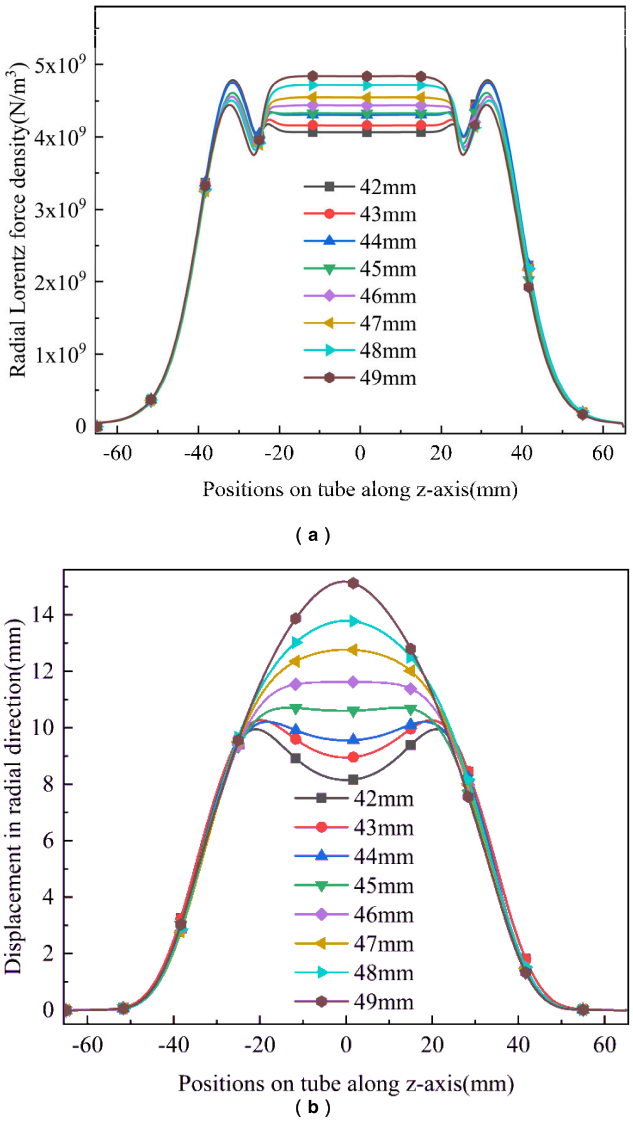

FIGURE 9. Influence of H_i variation on the (a) radial electromagnetic force, (b) deformation behavior.

2) INFLUENCE OF H_o

Figure 10(a) shows the effect of the height of the outer wall of the magnetic field shaper on the radial-electromagnetic force. In contrary to the effect of H_i, one can observe that when H_o decreases, the radial-electromagnetic force decreases at the middle section while the electromagnetic force at the end of the magnetic field shaper exhibits a substantial change.

Figure 10(b) shows the effect of H_o variation on the pipe deformation performance in the radial direction. Results show that with the increase of H_o, the bulging profile of the pipe changes from convex to concave. This is mainly because when the height of the outer wall of the magnetic field shaper increases, the deformation area of the pipe becomes wider and the magnetic field in the middle of the pipe is weakened too much. As a result, the deformation area in the middle is not fully bulged. In this example, the outer wall height of the best magnetic field shaper to achieve uniform bulging is 49mm.

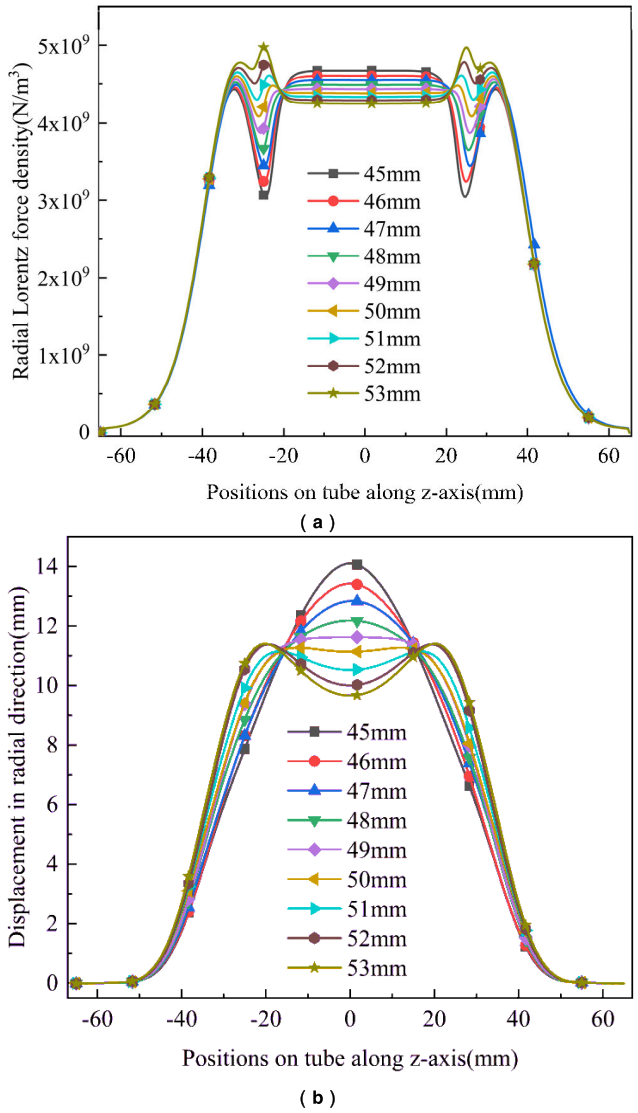

FIGURE 10. Effect of H_o on (a) radial electromagnetic force, (b) deformation behavior.

The above analysis shows that introducing a magnetic field shaper between the driving coil and the metal pipe can effectively change the induced eddy-current in the deformation area of the pipe, thereby regulating the electromagnetic force distribution of the pipe, and making the pipe more uniform in the axial direction. For the considered case study, the optimum values of H_i and H_o are 46mm and 49mm, respectively.

B. COMPARATIVE INVESTIGATION

To reveal the advantages of the magnetic field shaper-based loading method, this section compares the performance of tube EMF based on traditional and the magnetic field convert methods. Considered performance metrics include the magnetic field pressure, axial magnetic flux, radial-electromagnetic force, and tube deformation performance. Table 3 shows the geometrical dimensions of the traditional cylindrical coil and the proposed magnetic field shaper. The

TABLE 3. Geometric parameters of the analyzed traditional and the proposed magnetic field shaper- based EMF (in mm).

		Height	Inner radius	Outer radius
Traditional		80	30.2	36.2
	Bulging coil	80	23	29
Proposed				
	Inner wall	46	30.2	
	Outer wall	49		36.2

workpiece is an AA5083-O aluminum alloy tube with a length of 130mm, 37.5mm diameter and 2mm thickness. For precise comparison, the discharging voltage is considered as 3.98kV for traditional cylindrical coil and 6.4kV for the magnetic field shaper to warrant the same maximum pipe deformation under the two loading methods. Fig. 11 shows the three-dimensional (3D) distribution of the radial magnetic field pressure with time and axial position for the traditional cylindrical coil and the proposed magnetic field shaper EMF methods. It can be seen that the 3D cloud image of the magnetic field pressure of the traditional cylindrical coil exhibits a cone distribution with maximum value at the middle of the pipe. However, when the proposed magnetic field shaper is used for loading, the radial magnetic field pressure distribution becomes wider and more dispersed. This can effectively increase the magnetic-field at the end of the pipe and improve the distribution of the radial- electromagnetic force in the axial direction of the pipe.

In order to better illustrate that the electromagnetic bulging of tube based on the proposed method can improve the forming uniformity, a 3D graph of the distribution of the eddy current induced on the inner wall of the magnetic field shaper over time is obtained as shown in Figure 12. When a traditional coil is used to load the pipe, the driving coil is cylindrically wound and the same driving current is passed. Due to the uniform current distribution, the induced current in the axial direction of the pipe is also uniformly distributed. On the other hand, when the proposed magnetic field shaper is employed for loading, the distribution of the induced eddy current at the end of the magnetic field shaper is obviously increasing. Therefore, the magnetic field on the middle of the pipe is weakened, so that the radial electromagnetic force in the axial direction of the pipe is distributed in a concave shape, which improves the uniformity of the pipe forming.

The axial flux density and the corresponding radial electromagnetic force distributions are obtained as shown in Figs. 13 and 14 when conventional coil and the proposed loading methods are used. When a traditional coil is used, the radial electromagnetic force is distributed in a convex profile, and the end effect is obvious. When the proposed magnetic field

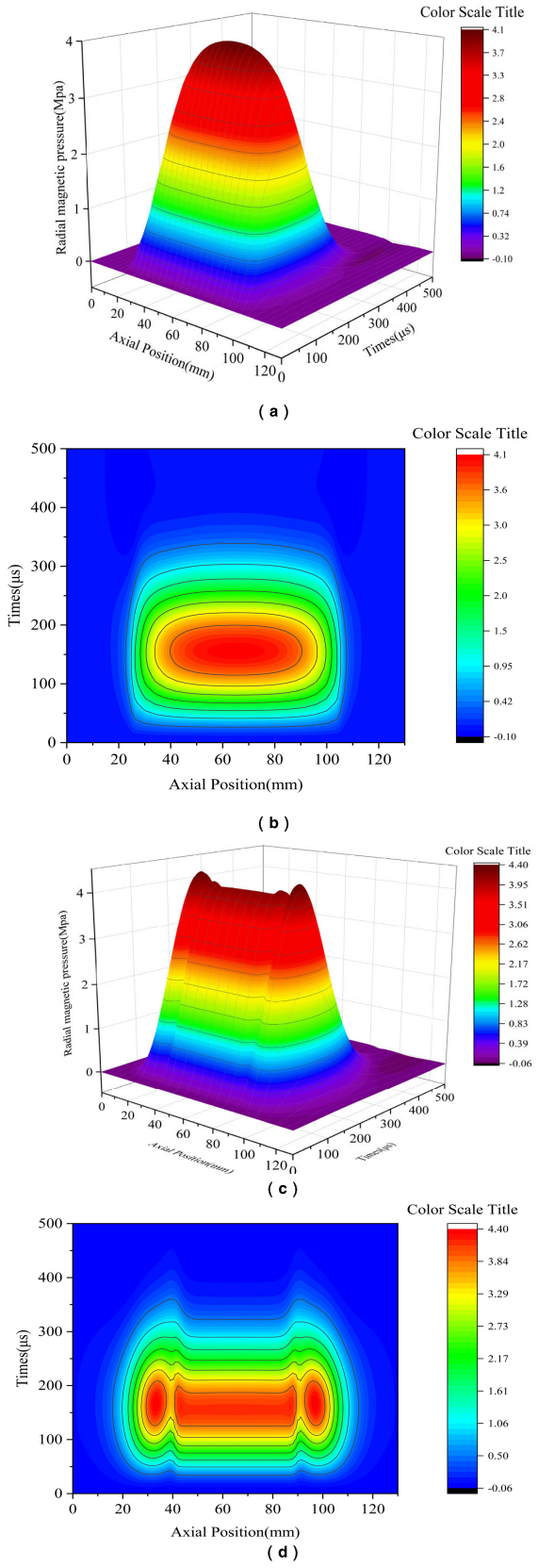

FIGURE 11. Distribution of radial magnetic pressure with time and axial position (a), (c) 3D cloud image of traditional and the proposed method; (b), (d) Top view of traditional and the proposed method.

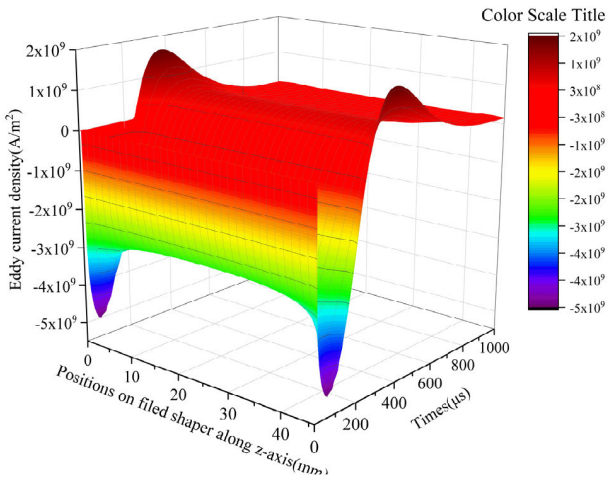

FIGURE 12. Distribution of induced eddy current with time and axial position.

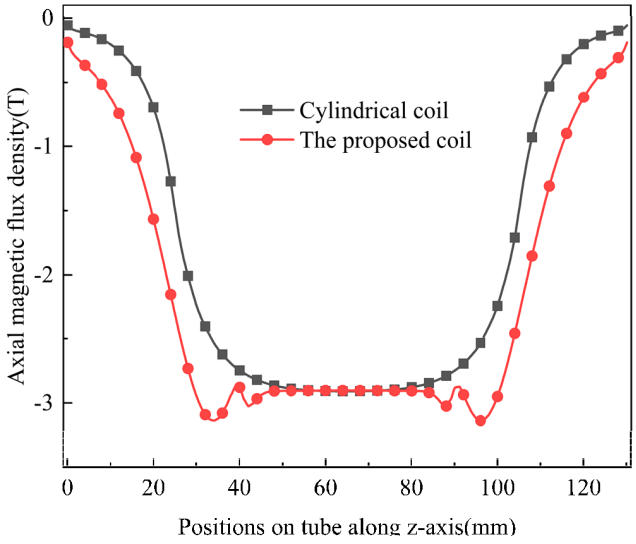

FIGURE 13. Axial distribution of the axial magnetic-flux density for the two driving coils topologies.

shaper is used for loading, the radial electromagnetic force presents a concave distribution, and the electromagnetic force in the middle of the pipe is obviously weakened. In addition, the electromagnetic force influence area becomes wider, which results is in increased forming amount of the end of the pipe.

Fig. 15 shows the radial displacement of the tube in the axial direction when the two EMF methods are employed. It can be seen that when the traditional spiral coil is used for loading, the deformation of the pipe in the axial direction is convexly distributed, the middle of the pipe has the largest deformation, and the two ends of the pipe have little deformation. This phenomenon is caused due to the radial electromagnetic force distribution in Fig. 14. When the loading method proposed in this paper is adopted, the radial deformation of

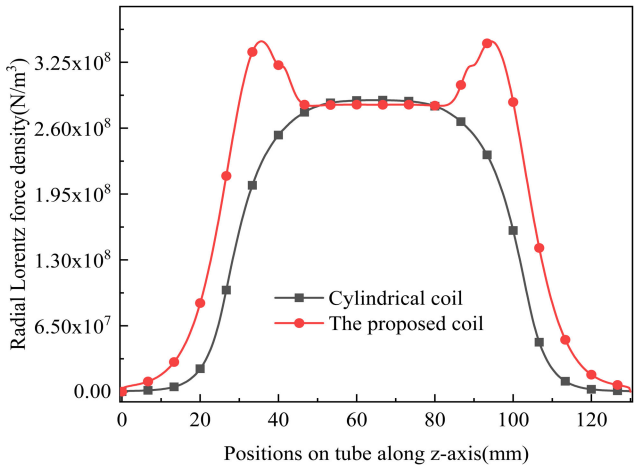

FIGURE 14. Radial electromagnetic-force profiles for the two coils.

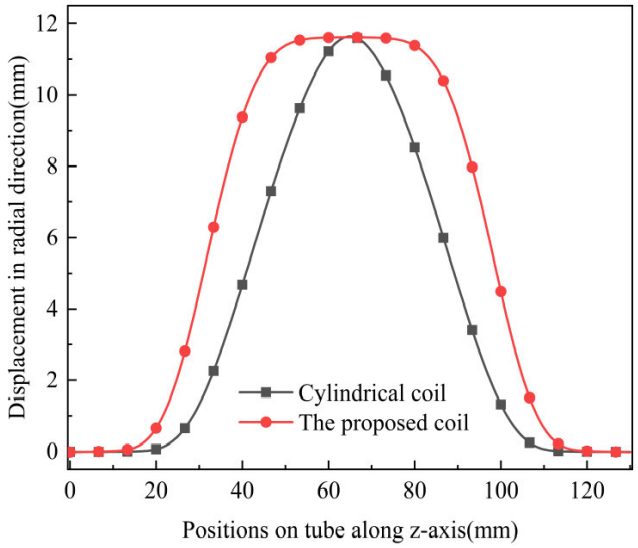

FIGURE 15. The amount of deformation along the axial direction of the pipe under different loading methods.

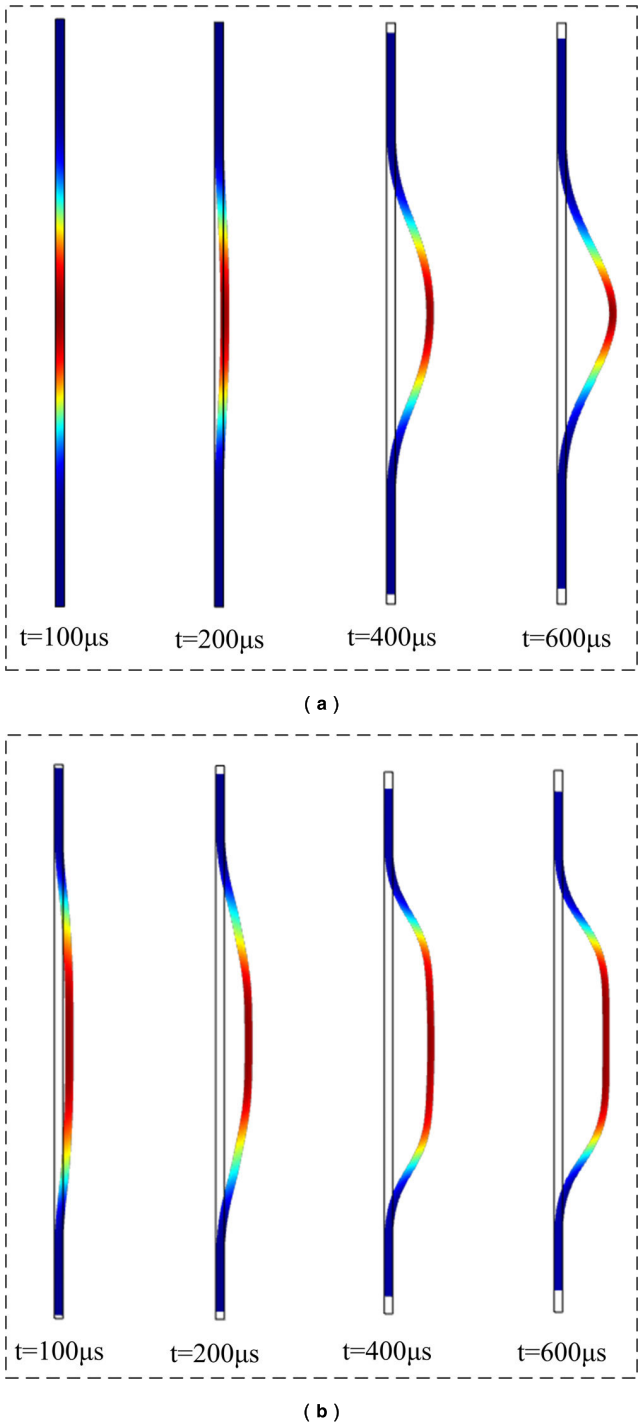

FIGURE 16. Tube forming conditions at different times. (a) Traditional cylindrical coil. (b) Proposed magnetic field shaper.

the pipe has a relatively flat top and the deformation area of the pipe becomes wider. Obviously, the end effect of the electromagnetic bulging of the traditional helical coil tube is weakened to a certain extent.

Furthermore, in order to better reflect the deformation state of the pipe fitting during the expansion process, the forming conditions of the pipe fitting at different times when using the conventional coil and magnetic field shaper proposed in this paper are obtained as shown in Figure 16. It can be seen that at t = 100μs, when the conventional cylindrical coil is loaded, the middle part of the tube begins to deform, and the deformation area of the driving coil based on the magnetic field shaper is larger. At t = 600μs, the tube reaches a maximum deformation, and when the traditional cylindrical coil is loaded, the axial deformation of the tube is uneven and exhibits a convex distribution. When the proposed topology is employed, the tube is uniformly deformed and the flow of the tube material in the axial direction can be realized.

In order to evaluate the uniformity of the pipe free bulging under different loading methods, this paper introduces a mathematical metric defined as the maximum uniform bulging range D_r that represents the axial length with a deformation greater than or equal to 96% of the maximum

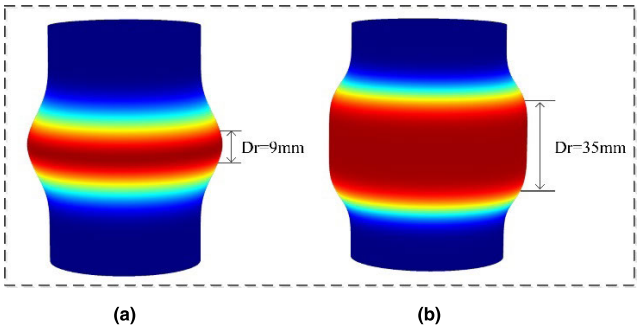

FIGURE 17. 3D contour of tube forming: (a) Traditional cylindrical coil; (b) Proposed magnetic field shaper.

deformation. Figure 17 shows a three-dimensional contour diagram of the pipe free bulging under the two loading methods. It can be seen that when the traditional helical coil is used for loading, D_r is 9mm, and the uniform range is small and located in the middle section of the pipe. On the other hand, when the loading method proposed in this paper is used, D_r becomes 35mm and the bulging area is becoming significantly wider. In contrast, the maximum uniform range is increased by 2.89 times. Obviously, the electromagnetic bulging of tubes based on the proposed magnetic field shaper can solve the existing dilemma of pipe deformation.

V. CONCLUSION

To solve the problem of uneven axial deformation of the existing tube electromagnetic bulging, this paper presents an EMF technology using a magnetic field shaper. Numerical results reveal that when the proposed method is employed, the radial-electromagnetic force becomes of concave-distribution which can significantly increase the end deformation of the pipe fitting, overcome the end effect of the conventional forming process of pipe fitting, and make the axial deformation of pipe fitting more uniform. Results also show that when the system discharge parameters remain unchanged, there is a suitable magnetic field shaper structure parameter that optimize the electromagnetic forming the pipe fitting. In addition, when the internal bulging amount of the pipe is the same, by introducing a magnetic field shaper between the driving coil and the pipe, the distribution of the induced eddy current in the pipe can be effectively adjusted, thereby realizing the loading of different electromagnetic force distributions. Numerical comparative analysis show that uniformity of the tube using the proposed magnetic field shaper can be improved by nearly 3.9 times compared with the traditional cylindrical coil loading.

REFERENCES

[1] S. Ouyang, X. Li, C. Li, L. Du, T. Peng, X. Han, L. Li, Z. Lai, and Q. Cao, "Investigation of the electromagnetic attractive forming utilizing a dual-coil system for tube bulging," *J. Manuf. Processes*, vol. 49, pp. 102–115, Jan. 2020.

[2] Q. Cao, L. Du, Z. Li, Z. Lai, Z. Li, M. Chen, X. Li, S. Xu, Q. Chen, X. Han, and L. Li, "Investigation of the Lorentz-force-driven sheet metal stamping process for cylindrical cup forming," *J. Mater. Process. Technol.*, vol. 271, pp. 532–541, Sep. 2019.

[3] L. Qiu, W. Zhang, A. Abu-Siada, Q. Xiong, C. Wang, Y. Xiao, B. Wang, Y. Li, J. Jiang, and Q. Cao, "Electromagnetic force distribution and wall thickness reduction of three-coil electromagnetic tube bulging with axial compression," *IEEE Access*, vol. 8, pp. 21665–21675, 2020, doi: 10.1109/ACCESS.2020.2969678.

[4] L. Qiu, B. Wang, A. Abu-Siada, Q. Xiong, W. Zhang, W. Ge, C. Liu, L. Jiang, and C. Wang, "Research on forming efficiency in double-sheet electromagnetic forming process," *IEEE Access*, vol. 8, pp. 19248–19255, 2020, doi: 10.1109/ACCESS.2020.2968049.

[5] L. Qiu, N. Yi, A. Abu-Siada, J. Tian, Y. Fan, K. Deng, Q. Xiong, and J. Jiang, "Electromagnetic force distribution and forming performance in electromagnetic forming with discretely driven rings," *IEEE Access*, vol. 8, pp. 16166–16173, 2020., doi: 10.1109/ACCESS.2020.2967096.

[6] L. Qiu, C. Wang, A. Abu-Siada, Q. Xiong, W. Zhang, B. Wang, N. Yi, Y. Li, and Q. Cao, "Coil temperature rise and workpiece forming efficiency of electromagnetic forming based on half-wave current method," *IEEE Access*, vol. 8, pp. 9371–9379, 2020, doi: 10.1109/ACCESS.2020.2965254.

[7] L. Huang, J. Zhang, J. Zou, Y. Zhou, and L. Qiu, "Effect of equivalent radius of drive coil on forming depth in electromagnetic sheet free bulging," *Int. J. Appl. Electromagn. Mech.*, vol. 61, no. 3, pp. 377–389, Nov. 2019.

[8] Q. Cao, Z. Li, Z. Lai, Z. Li, X. Han, and L. Li, "Analysis of the effect of an electrically conductive die on electromagnetic sheet metal forming process using the finite element-circuit coupled method," *Int. J. Adv. Manuf. Technol.*, vol. 101, nos. 1–4, pp. 549–563, Mar. 2019.

[9] X. Zhang, Q. Cao, X. Han, Q. Chen, Z. Lai, Q. Xiong, F. Deng, and L. Li, "Application of triple-coil system for improving deformation depth of tube in electromagnetic forming," *IEEE Trans. Appl. Supercond.*, vol. 26, no. 4, pp. 1–4, Jun. 2016, Art. no. 3701204, doi: 10.1109/TASC.2016.2542482.

[10] Q. Cao, Z. Lai, Q. Xiong, Q. Chen, T. Ding, X. Han, and L. Li, "Electromagnetic attractive forming of sheet metals by means of a dual-frequency discharge current: Design and implementation," *Int. J. Adv. Manuf. Technol.*, vol. 90, nos. 1–4, pp. 309–316, Apr. 2017.

[11] M. Geier, E. Paese, R. Rossi, P. A. R. Rosa, and R. P. Homrich, "Experimental analysis of interference-fit joining of aluminum tubes by electromagnetic forming," *IEEE Trans. Appl. Supercond.*, vol. 30, no. 4, pp. 1–6, Jun. 2020, Art. no. 0600306, doi: 10.1109/TASC.2020.2972499.

[12] L. Qiu, Y. Li, Y. Yu, Y. Xiao, P. Su, Q. Xiong, J. Jiang, and L. Li, "Numerical and experimental investigation in electromagnetic tube expansion with axial compression," *Int. J. Adv. Manuf. Technol.*, vol. 104, nos. 5–8, pp. 3045–3051, Oct. 2019.

[13] L. Qiu, K. Deng, Y. Li, X. Tian, Q. Xiong, P. Chang, P. Su, and L. Huang, "Analysis of coil temperature rise in electromagnetic forming with coupled cooling method," *Int. J. Appl. Electromagn. Mech.*, vol. 63, no. 1, pp. 45–58, May 2020, doi: 10.3233/JAE-190062.

[14] L. Qiu, Y. Yu, Y. Yang, X. Nie, Y. Xiao, Y. Ning, F. Wang, and C. Cao, "Analysis of electromagnetic force and experiments in electromagnetic forming with local loading," *Int. J. Appl. Electromagn. Mech.*, vol. 57, no. 1, pp. 29–37, Apr. 2018.

[15] H.-P. Yu, C.-F. Li, D.-H. Liu, and X. Mei, "Tendency of homogeneous radial deformation during electromagnetic compression of aluminium tube," *Trans. Nonferrous Metals Soc. China*, vol. 20, no. 1, pp. 7–13, Jan. 2010.

[16] N. Liu, Z. Lai, Q. Cao, X. Han, Y. Huang, X. Li, M. Chen, and L. Li, "A comparative study on the effects of boundary constraints on electromagnetic sheet forming," *Int. J. Adv. Manuf. Technol.*, vol. 101, nos. 9–12, pp. 2785–2793, Apr. 2019.

[17] Z. Wu, Q. Cao, J. Fu, Z. Li, Y. Wan, Q. Chen, L. Li, and X. Han, "An inner-field uniform pressure actuator with high performance and its application to titanium bipolar plate forming," *Int. J. Mach. Tools Manuf.*, vol. 155, May 2020, Art. no. 103570.

[18] Q. Zhang, L. Huang, J. Li, F. Feng, H. Su, F. Ma, and K. Zhong, "Investigation of dynamic deformation behaviour of large-size sheet metal parts under local Lorentz force," *J. Mater. Process. Technol.*, vol. 265, pp. 20–33, Mar. 2019.

[19] L. Qiu, Y. Li, Y. Yu, A. Abu-Siada, Q. Xiong, X. Li, L. Li, P. Su, and Q. Cao, "Electromagnetic force distribution and deformation homogeneity of electromagnetic tube expansion with a new concave coil structure," *IEEE Access*, vol. 7, pp. 117107–117114, 2019.

[20] S. Golowin, M. Kamal, J. Shang, J. Portier, A. Din, G. S. Daehn, J. R. Bradley, K. E. Newman, and S. Hatkevich, "Application of a Uniform Pressure Actuator for Electromagnetic Processing of Sheet Metal," *J. Mater. Eng. Perform.*, vol. 16, no. 4, pp. 455–460, 2007.

[21] Z. Jian *et al.*, "Numerical simulation and forming uniformity of electromagnetic progressive bulging of tube," *J. Plasticity Eng.*, vol. 19, no. 5, pp. 92–99, 2012.
[22] R. Chaharmiri and A. F. Arezoodar, "The effect of stepped field shaper on magnetic pressure and radial displacement in electromagnetic inside bead forming: Experimental and simulation analyses using Maxwell and Abaqus software," *J. Manuf. Sci. Eng.*, vol. 139, no. 6, p. 61003, Jun. 2017.
[23] M. A. Bahmani, K. Niayesh, and A. Karimi, "3D simulation of magnetic field distribution in electromagnetic forming systems with field-shaper," *J. Mater. Process. Technol.*, vol. 209, no. 5, pp. 2295–2301, Mar. 2009.
[24] D. S. K, M. R. Kulkarni, S. Kumar, P. C. Saroj, and A. Sharma, "Magnetic field enhancement using field shaper for electromagnetic welding system," in *Proc. IEEE Appl. Electromagn. Conf. (AEMC)*, Dec. 2015.
[25] Q. Xiong, H. Huang, C. Deng, L. Li, L. Qiu, and H. Tang, "A method to improve forming accuracy in electromagnetic forming of sheet metal," *Int. J. Appl. Electromagn. Mech.*, vol. 57, no. 3, pp. 367–375, Jun. 2018.
[26] Y.-Y. Chu and R.-S. Lee, "Effect of field shaper geometry on the Lorentz force for electromagnetic sheet impact forming process," *Proc. Inst. Mech. Eng. B, J. Eng. Manuf.*, vol. 227, no. 2, pp. 324–332, Feb. 2013.
[27] Q. Cao, X. Han, Z. Lai, Q. Xiong, X. Zhang, Q. Chen, H. Xiao, and L. Li, "Analysis and reduction of coil temperature rise in electromagnetic forming," *J. Mater. Process. Technol.*, vol. 225, pp. 185–194, Nov. 2015.
[28] Q. Cao, X. Han, Z. Lai, B. Zhang, Z. Zhou, L. Qiu, and L. Li, "Effects of current frequency on electromagnetic sheet metal forming process," *IEEE Trans. Appl. Supercond.*, vol. 24, no. 3, Jun. 2014, Art. no. 3700104.
[29] L. Qiu, C. Wang, A. Abu-Siada, W. Bin, Z. Wang, W. Ge, C. Liu, and P. Chang, "Parametric simulation analysis of the electromagnetic force distribution and formability of tube electromagnetic bulging based on auxiliary coil," *IEEE Access*, vol. 8, pp. 159979–159989, 2020, doi: 10.1109/ACCESS.2020.3020830.
[30] L. Qiu, K. Deng, A. Abu-Siada, Q. Xiong, N. Yi, Y. Fan, J. Tian, and J. Jiang, "Construction and analysis of two-dimensional axisymmetric model of electromagnetic tube bulging with field shaper," *IEEE Access*, vol. 8, pp. 113713–113719, 2020, doi: 10.1109/ACCESS-.2020.3003740.
[31] L. Qiu, W. Zhang, A. Abu-Siada, G. Liu, C. Wang, Y. Wang, B. Wang, Y. Li, and Y. Yu, "Analysis of electromagnetic force and formability of tube electromagnetic bulging based on convex coil," *IEEE Access*, vol. 8, pp. 33215–33222, 2020, doi: 10.1109/ACCESS.2020.2974758.

LI QIU (Member, IEEE) received the B.S., M.S., and Ph.D. degrees in electrical engineering from the Huazhong University of Science and Technology, Wuhan, China, in 2012. He is currently an Associate Professor with the College of Electrical Engineering and New Energy, China Three Gorges University, Yichang. He has authored more than 15 articles and holds more than ten inventions. His research interests include the technology of pulsed high-magnetic field, high-voltage technology, and electromagnetic forming. He is Periodical Reviewer of the IEEE TRANSACTIONS ON APPLIED SUPERCONDUCTIVITY and the *International Journal of Applied Electromagnetics and Mechanics*.

CHENGLIN WANG was born in Sichuan, China, in 1996. He received the bachelor's degree from the College of Information Science and Engineering, Chengdu University, Chengdu, China, in 2019. He is currently pursuing the master's degree in electrical engineering with the College of Electrical Engineering and New Energy, China Three Gorges University, Yichang.

AHMED ABU-SIADA (Senior Member, IEEE) received the B.Sc. and M.Sc. degrees from Ain Shams University, Egypt, in 1998, and the Ph.D. degree from Curtin University, Australia, in 2004, all in electrical engineering. He is currently an Associate Professor and the Discipline Lead of Electrical and Computer Engineering with Curtin University. His research interests include power electronics, power system stability, condition monitoring, and power quality. He is the Vice-Chair of the IEEE Computation Intelligence Society and WA Chapter. He is the Editor-in-Chief of the *International Journal of Electrical and Electronics Engineering* and a regular Reviewer of various IEEE TRANSACTIONS.

WANG BIN is currently pursuing the degree in electrical engineering with the College of Electrical Engineering and New Energy, China Three Gorges University, Yichang.

ZHANG WANG is currently pursuing the degree in electrical engineering with the College of Electrical Engineering and New Energy, China Three Gorges University, Yichang.

WEIKANG GE is currently pursuing the degree in electrical engineering with the College of Electrical Engineering and New Energy, China Three Gorges University, Yichang.

CHANG LIU is currently pursuing the master's degree in electrical engineering with the College of Electrical Engineering and New Energy, China Three Gorges University, Yichang.

YUWEI FAN is currently pursuing the degree in electrical engineering with the College of Electrical Engineering and New Energy, China Three Gorges University, Yichang.